The mitotic spindle mediates inheritance of the Golgi ribbon structure

Jen-Hsuan Wei and Joachim Seemann

Department of Cell Biology, University of Texas Southwestern Medical Center, Dallas, TX 75390

The mammalian Golgi ribbon disassembles during mitosis and reforms in both daughter cells after division. Mitotic Golgi membranes concentrate around the spindle poles, suggesting that the spindle may control Golgi partitioning. To test this, cells were induced to divide asymmetrically with the entire spindle segregated into only one daughter cell. A ribbon reforms in the nucleated karyoplasts, whereas the Golgi stacks in the cytoplasts are scattered. However, the scattered Golgi stacks are polarized and transport cargo. Microinjection of Golgi extract together with tubulin or incorporation of spindle materials rescues Golgi ribbon formation. Therefore, the factors required for postmitotic Golgi ribbon assembly are transferred by the spindle, but the constituents of functional stacks are partitioned independently, suggesting that Golgi inheritance is regulated by two distinct mechanisms.

Introduction

The Golgi apparatus in mammalian cells consists of stacks of flattened cisternae that are linked together laterally into a single continuous ribbon in the perinuclear region. As the central hub of the secretory pathway, the Golgi receives newly synthesized proteins from the ER and sorts them into their correct cellular destinations. The orientation of the Golgi ribbon directs exocytosis toward a particular area of the plasma membrane and thereby facilitates the establishment of cell polarity, for instance, during wound healing (Preisinger et al., 2004), neural development (Horton et al., 2005), and immune response (Stinchcombe et al., 2006).

During cell division, the single Golgi ribbon needs to be segregated into the two daughter cells. To achieve partitioning, the Golgi fragments at the onset of mitosis, and later reforms in each daughter cell (for review see Lowe and Barr, 2007). Two different mechanisms have been proposed for the partitioning of the Golgi. In one view, Golgi membranes are absorbed into and partitioned with the ER (Zaal et al., 1999). The second view argues that the Golgi remains distinct from the ER and that the two compartments are inherited independently (Bartz and Seemann, 2008). In this scenario, the spindle has been proposed as the machinery responsible for Golgi partitioning based on the observed accumulation of Golgi membranes at the spindle poles (Shima et al., 1998), although a pool of membranes is dispersed throughout the cytoplasm (Jesch et al., 2001).

To elucidate the role of the spindle in Golgi partitioning, we established an assay in which the entire spindle is segregated into only one daughter cell. Upon division, a Golgi ribbon reformed in the karyoplasts, whereas the stacked cisternae were scattered throughout the cytoplasts. We could rescue ribbon assembly in the cytoplasts by microinjecting the Golgi extract together with tubulin or by lowering the division temperature, at which partial spindle materials were transferred into the cytoplasts. We propose that Golgi factors required for ribbon assembly rely on the spindle for partitioning, but functional stacks are inherited independently. This reveals two levels of regulation underlying Golgi inheritance. Coupling of these factors with the spindle would ensure that daughter cells receive the information to assemble the Golgi ribbon, which is vital for cellular functions that require polarized secretion and directional migration.

Results and discussion

To evaluate the role of the spindle in Golgi partitioning, we first examined the spatial correlation between Golgi membranes and the spindle. Consistent with previous studies (Shima et al., 1998; Jokitalo et al., 2001), we found Golgi membranes concentrated in metaphase around the two spindle poles in a variety of cell lines, including HeLa, Vero, LLC-PK1, normal rat kidney, and PtK1 (unpublished data). The association was prominent in

Correspondence to Joachim Seemann: joachim.seemann@utsouthwestern.edu

Abbreviations used in this paper: NAGT I, *N*-acetylglucosaminyl transferase I; PDI, protein disulfide isomerase; RLG, rat liver Golgi.

© 2009 Wei and Seemann This article is distributed under the terms of an Attribution–Noncommercial–Share Alike–No Mirror Sites license for the first six months after the publication date (see http://www.jcb.org/misc/terms.shtml). After six months it is available under a Creative Commons License (Attribution–Noncommercial–Share Alike 3.0 Unported license, as described at http://creativecommons.org/licenses/by-nc-sa/3.0/).

The Rockefeller University Press $30.00
J. Cell Biol. Vol. 184 No. 3 391–397
www.jcb.org/cgi/doi/10.1083/jcb.200809090

THE JOURNAL OF CELL BIOLOGY

Downloaded from http://rupress.org/jcb/article-pdf/184/3/391/1897081/jcb_200809090.pdf by guest on 09 February 2026

PtK1 cells and was observed for both the stably expressed GFP-tagged Golgi enzyme *N*-acetylglucosaminyl transferase I (NAGT I) and the endogenous Golgi matrix protein GM130 (Fig. 1, B and C). We occasionally observed aberrant monopolar, tripolar, and tetrapolar spindles and Golgi membranes clustered at the spindle poles as well (Fig. 1, D–F). Moreover, accumulation of Golgi at the spindle poles was still evident when PtK1 cells were treated with the Eg5 inhibitors monastrol (Mayer et al., 1999) or trityl-cysteine (Skoufias et al., 2006) to induce monopolar spindles (Fig. 1, G and H). Collectively, these data suggest a robust association of mitotic Golgi membranes with the spindle apparatus.

To test whether the spindle is required for Golgi partitioning, we established a system in which mitotic cells were induced to divide asymmetrically into two daughter cells, but only one of which received the entire spindle (Fig. 2 A). PtK1 cells stably expressing NAGT I–GFP were treated with an Eg5 inhibitor, either monastrol or trityl-cysteine. Upon entry into mitosis, inhibition of the kinesin Eg5 blocks centrosome separation, leading to the formation of monoasters and the arrest of cells in M phase (Mayer et al., 1999). Monoasters consist of microtubules emanating from nonseparated centrosomes and are surrounded by condensed chromosomes. Because PtK1 cells remain relatively flat during mitosis, monoasters are often asymmetrically located at one side of the cells (Canman et al., 2003). We induced cell division by two independent methods. We microinjected recombinant Mad1 to sequester Mad2 from the kinetochores, which silences the spindle checkpoint and allows progression through mitosis (Canman et al., 2003). We also found that asymmetrical cell division could be induced by inhibition of Cdk1 with roscovitine or purvalanol A (Niiya et al., 2005; Hu et al., 2008). Both approaches generated a cytoplast without a nucleus and a nucleated karyoplast. Daughter cells were either identified by the injection marker (Mad1 injection) or monitored by time-lapse phase-contrast microscopy (Cdk1 inhibition).

After division, the karyoplasts received the chromosomes (Fig. 2, E and I), centrosomes (unpublished data), and microtubules (Fig. 2, D and H), whereas the cytoplasts lacked all of these. Intriguingly, Golgi markers, including NAGT I–GFP and GM130, were detected in both cells (Fig. 2, C and G), suggesting that parts of the Golgi were partitioned independently of the spindle ($n = 29$ for Mad1 injection; and $n > 50$ for Cdk1 inhibition). However, the organization of the Golgi in the two daughter cells was very different. We analyzed the Golgi distribution in each daughter cell, where the Golgi was determined as a ribbon if 90% of the fluorescence resided in no more than three continuous structures (Puthenveedu et al., 2006). The Golgi in the karyoplasts localized to the perinuclear region and exhibited the characteristic ribbon structure (Fig. 2, C and G). In contrast, the Golgi in the cytoplasts was spread throughout the cytoplasm and failed to reform a ribbon (Fig. 2, C and G). This indicates that the spindle has a direct role in inheritance of the Golgi ribbon.

To eliminate the possibility that the scattered Golgi in the cytoplasts might be caused by cell death, we followed both karyoplasts and cytoplasts by video microscopy. The cytoplasts

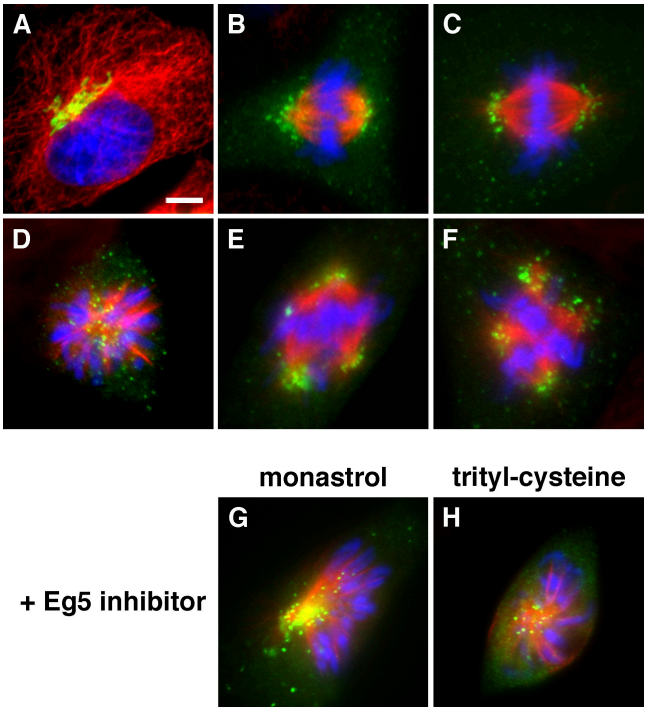

Figure 1. **Mitotic Golgi membranes accumulate at the spindle poles.** (A–H) PtK1 cells were stained for the Golgi resident enzyme NAGT I–GFP (A and B) or the Golgi matrix protein GM130 (C–H; green), tubulin (red), and DNA (blue). Upon entry into mitosis, the Golgi ribbon (A) was disassembled into vesicles that clustered around the spindle poles in metaphase (B and C). Mitotic Golgi membranes concentrated at the spindle poles in cells containing monopolar (D), tripolar (E), or tetrapolar (F) spindles as well as in cells with monopolar spindles induced by an Eg5 inhibitor, either monastrol (G) or trityl-cysteine (H). Bar, 4 µm.

survived on average 36 h after division and, in some cases, were still alive and seemingly healthy when corresponding karyoplasts underwent a second round of cell division.

The scattered Golgi and the absence of microtubules in the cytoplasts are reminiscent of cells treated with nocodazole, which causes the Golgi ribbon to fragment into stacks that are dispersed throughout the cell (Shima et al., 1998). Our EM analysis revealed that the Golgi in both karyoplasts and cytoplasts was stacked with an average of 3.4 ± 0.7 (karyoplast; $n = 22$) and 3.3 ± 0.6 (cytoplast; $n = 23$) cisternae per stack (Fig. 3, A and B). The cisternae were stacked to a comparable extent and separated by 11.8 ± 3.8 (karyoplast) and 12.9 ± 3.7 nm (cytoplast). To determine whether the stacks were polarized, we took advantage of a well-established fluorescence microscopy method (Shima et al., 1997). PtK1 cells stably expressing the medial/trans-Golgi enzyme NAGT I–GFP were induced to divide asymmetrically and immunolabeled for GFP and the cis-Golgi marker GM130 ($n = 15$). In these triple-labeled cells, the GFP fluorescence was first overlaid with the anti-GFP signal (Fig. 3, C and D) and was then overlaid with the anti-GM130 signal (Fig. 3, E and F). The anti-GFP staining served as a control, showing a complete overlap with the GFP fluorescence (Fig. 3, C and D). In contrast, the cis–anti-GM130 signal in the karyoplasts was found adjacent to the medial/trans-GFP fluorescence with only a partial overlap (Fig. 3 E), suggesting that the ribbon in the karyoplasts preserved a

Downloaded from http://rupress.org/jcb/article-pdf/184/3/391/1897081/jcb_200809090.pdf by guest on 09 February 2026

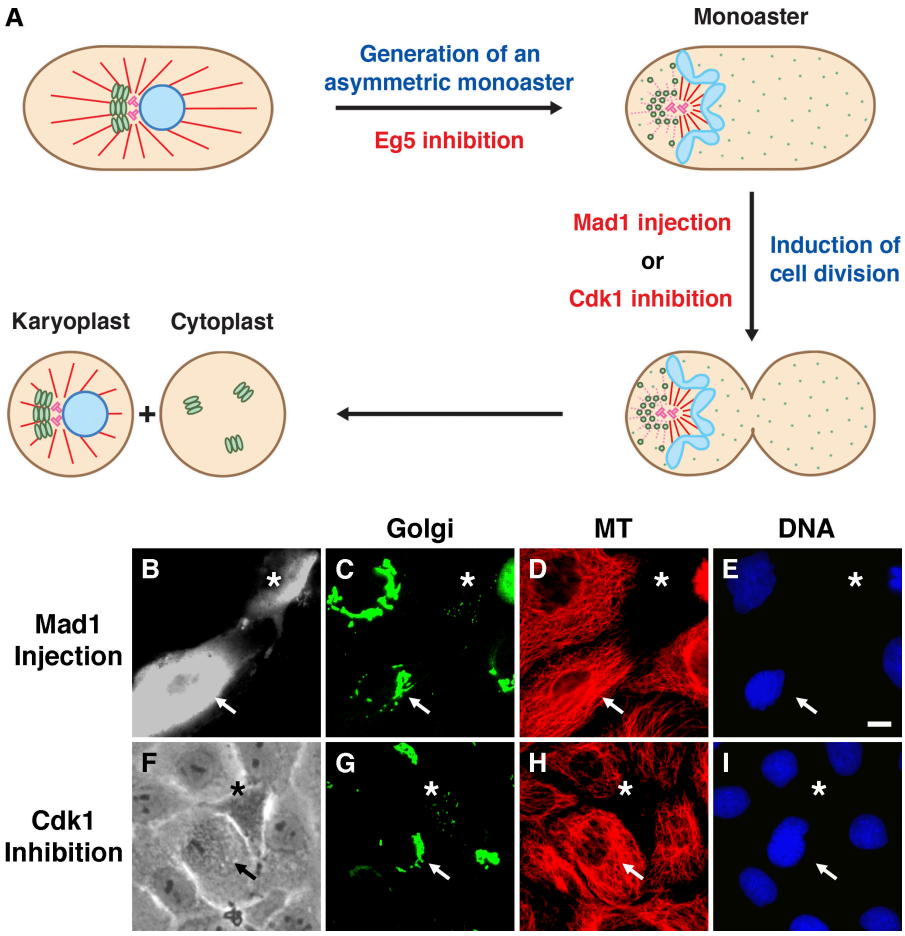

Figure 2. **The Golgi in the karyoplasts but not in the cytoplasts reforms a ribbon.** (A) Diagram of the assay. PtK1 cells stably expressing NAGT I–GFP were treated with an Eg5 inhibitor (monastrol or trityl-cysteine) for 2 h to induce asymmetrically positioned monoasters. Cell division was triggered either by microinjection of Mad1 or by addition of a Cdk1 inhibitor (purvalanol A or roscovitine), leading to a karyoplast that received the entire spindle (centrosomes, chromosomes, and spindle microtubules) and a cytoplast that lacked all of these. (B–I) Divided cells were either identified by the injection marker (B; Mad1 injection) or followed by time-lapse phase-contrast microscopy (F; Cdk1 inhibition). Cells were stained for GFP (C and G), tubulin (D and H), and DNA (E and I). The Golgi in the karyoplasts (arrows) reformed a characteristic ribbon in the perinuclear region, whereas the Golgi in the cytoplasts (asterisks) was scattered throughout the cytoplasm (C and G). In addition, no microtubule (MT) network was present in the cytoplasts (D and H). Bar, 10 μm.

cis-to-trans polarity. A similar segregation pattern was observed in the cytoplasts (Fig. 3 F). Together with our EM data, we conclude that the scattered Golgi in the cytoplasts is stacked and polarized.

We next investigated whether the stacked Golgi in the cytoplasts transports cargo. The mRNA of CD8, a plasma membrane protein not expressed in PtK1 cells, was injected together with Mad1 protein into cells with asymmetrical monoasters. Cells were incubated for 4 h to allow cell division, as well as synthesis and transport of cargo, and were fixed and stained before permeabilization. CD8 was detected on the cell surface in both karyoplasts and cytoplasts (n = 22; Fig. 3 H) but not in cells with impaired secretion (Fig. S1, available at http://www.jcb.org/cgi/content/full/jcb.200809090/DC1), indicating that the Golgi stacks in both cells transported cargo. To rule out that CD8 might have been expressed and transported before cytokinesis, we induced asymmetrical cell division in the presence of the protein synthesis inhibitor cycloheximide. After the drug was removed to allow protein expression and transport, CD8 was detected on the cell surface of both cells (n = 9; unpublished data). In another approach, we injected CD8 mRNA into the cytoplasts generated by Cdk1 inhibition. CD8 appeared on the cell surface of the cytoplasts but not on the noninjected karyoplasts (n = 8; Fig. 3 L). Similarly, myc-tagged protein A fused to the transmembrane domain of the PDGF receptor was also delivered to the cell surface (n = 15; Fig. S1 K). These findings indicate that the Golgi stacks in the cytoplasts are functional for secretion and do not require the spindle for partitioning.

In principle, the lack of a Golgi ribbon in the cytoplasts could be explained by two different mechanisms. First, the failure in ribbon assembly might be a result of the absence of microtubules in the cytoplasts because microtubules are essential to establish a Golgi ribbon. In this case, reformation of microtubules should restore the ribbon. Alternatively, the scattered Golgi stacks in the cytoplasts might be caused by the exclusion of the factors required for ribbon assembly (i.e., ribbon determinants). Ribbon determinants may associate with the spindle and are therefore not transferred to the cytoplasts. Supplying these factors should rescue ribbon formation. To distinguish between these two possibilities, we injected the missing materials into the cytoplasts and examined the Golgi morphology. Injection of tubulin resulted in a microtubule network (Fig. 4 C), demonstrating that the cellular environment in the cytoplasts supports microtubule polymerization (Pelletier et al., 2000). However, the overall organization of Golgi stacks remained scattered (n = 14, five independent experiments; Fig. 4 B), indicating that the microtubules in the cytoplasts are not sufficient to reassemble a ribbon. Therefore, additional factors might be required but were presumably segregated along with the spindle into the karyoplasts. Because these factors may associate with Golgi membranes, we extracted rat liver Golgi (RLG) membranes with the nonionic detergent n-octylglucoside and removed the

Downloaded from http://rupress.org/jcb/article-pdf/184/3/391/1897081/jcb_200809090.pdf by guest on 09 February 2026

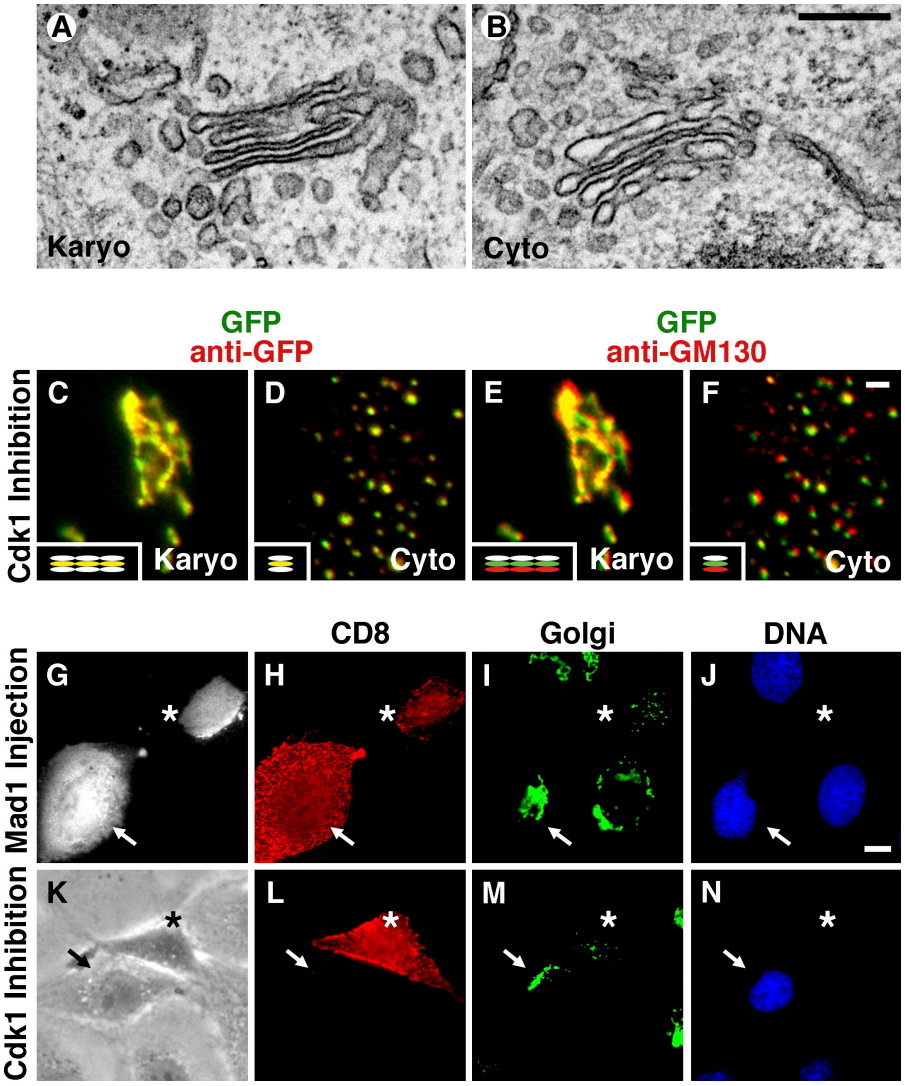

Figure 3. **The Golgi stacks in the cytoplasts are polarized and transport cargo.** (A–F) The Golgi in the cytoplasts is composed of polarized stacks. PtK1 cells stably expressing the medial/trans-Golgi enzyme NAGT I–GFP were induced to divide asymmetrically and followed by video microscopy. Upon division, cells were either processed for EM (A and B) or for immunofluorescence (C–F). (A and B) Stacked Golgi cisternae reformed in both karyoplasts (karyo; A) and cytoplasts (cyto; B). Bar, 200 nm. (C–F) The Golgi stacks are polarized. Divided cells were triple labeled with GFP, anti-GFP, and anti–cis-Golgi marker GM130. Two-channel overlays were performed as specified. GFP fluorescence is shown in green (C–F), and the antibody stainings for GFP (C and D) and GM130 (E and F) are pseudocolored in red. The GFP fluorescence colocalized with the anti-GFP signal (C and D) but only partially overlapped with the anti-GM130 signal (E and F) in both karyoplasts (C and E) and cytoplasts (D and F), as shown schematically in the insets. Bar, 2 µm. (G–N) CD8 transport assay. CD8 mRNA was microinjected into cells with asymmetrical monoasters together with Mad1 (G–J) or into the cytoplasts induced by Cdk1 inhibition (K–N). CD8 on the cell surface was stained before permeabilization (H and L). Note that CD8 was expressed and transported to the plasma membrane in the cytoplasts (asterisks). Karyoplasts are marked by arrows. Bar, 10 µm.

detergent by dialysis. Injection of Golgi extract alone had no effect ($n = 12$, four independent experiments; Fig. 4 F), but Golgi extract together with tubulin restored a ribbon ($n = 8$, five independent experiments; Fig. 4 J) as well as a microtubule network (Fig. 4 K). Thus, the factors required for ribbon assembly are located on the Golgi.

This is in line with previous studies showing that in cytoplasts generated by microsurgery, a Golgi ribbon forms in the absence of centrosomes but requires preexisting Golgi distributed into the cut cells under interphase condition (Maniotis and Schliwa, 1991; Pelletier et al., 2000). The mammalian Golgi ribbon is usually formed next to the centrosomes, which depends on the minus end–directed microtubule motor dynein. We did not detect centrosomes in serial sections of RLG membranes by EM. In addition, neither the centrosomal marker pericentrin nor cytoplasmic dynein were detectable by Western blotting in the RLG fraction, although the proteins were present in the homogenate (Fig. 4 N). Similarly, the ER enzyme protein disulfide isomerase (PDI) and the nuclear pore protein Nup153 were absent in the RLG fraction. In contrast, the Golgi proteins GM130 and GRASP65 were highly enriched. Interestingly, we found that medial/trans-Golgi markers were enriched in the Golgi extract, whereas cis-Golgi proteins were mostly depleted (Fig. 4 O). This implies that the factors required for postmitotic ribbon reassembly might have distinct molecular compositions from the cis-Golgi proteins Golgin84, GRASP65, and GM130 shown to be required for ribbon maintenance in interphase (Diao et al., 2003; Puthenveedu et al., 2006).

If the ribbon determinants are partitioned with the spindle, incorporation of parts of the spindle and its associated proteins into the cytoplasts should rescue ribbon formation. We followed asymmetrical cell division induced at lower temperature (32°C) and found that spindle positioning was dramatically altered, presumably caused by effects on microtubule dynamics (Fig. S2, available at http://www.jcb.org/cgi/content/full/jcb.200809090/DC1). At 37°C, the monopolar spindle was positioned distal to the cleavage furrow and seemingly adhered to the cortex at one side of the cell (Fig. 5 A and Video 1). The cytoplasts derived from this type of division contained scattered Golgi but no microtubules (Fig. 2, G and H; and Fig. 5, B and C). However, at a lower temperature, the spindle was positioned centrally in close proximity to the division plane (Fig. 5 E

Downloaded from http://rupress.org/jcb/article-pdf/184/3/391/1897081/jcb_200809090.pdf by guest on 09 February 2026

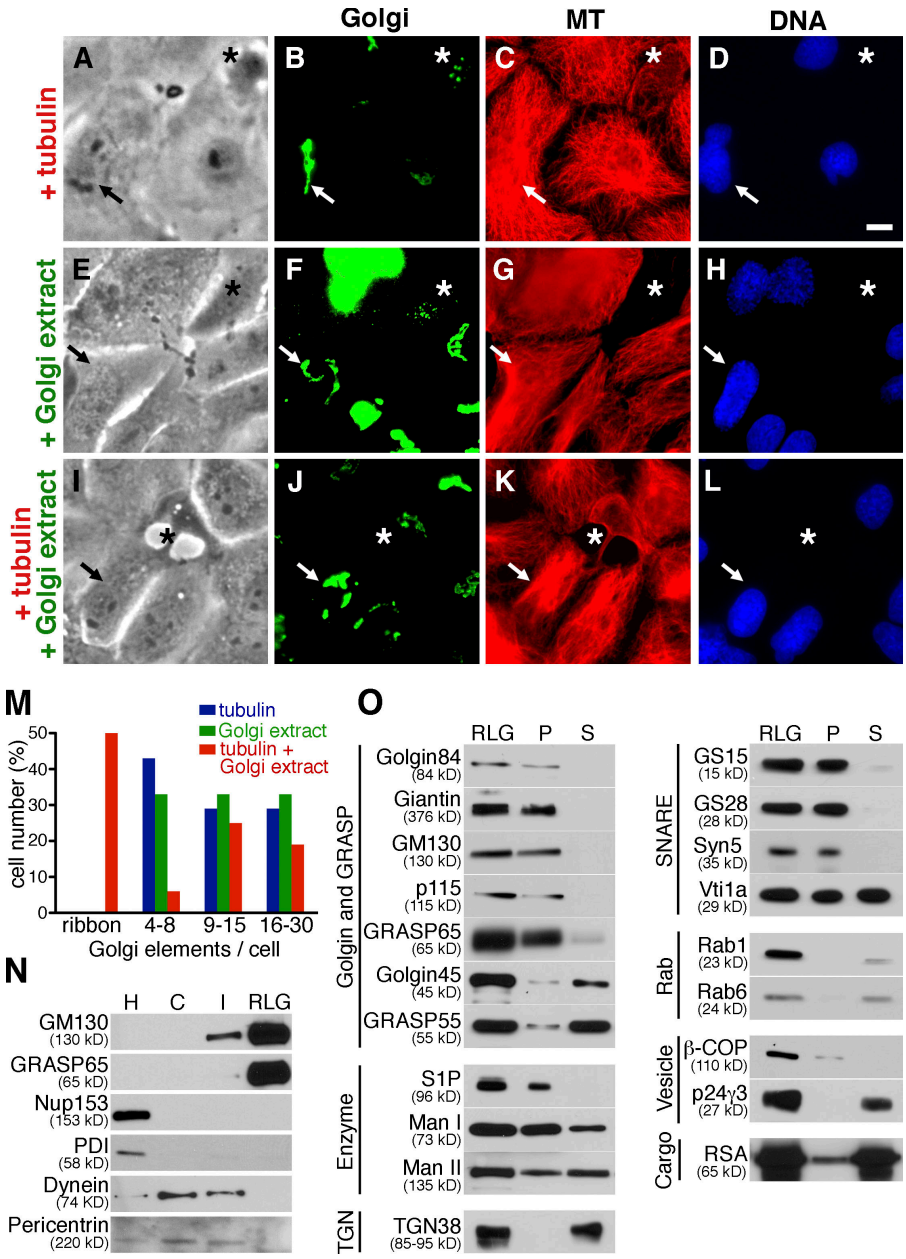

Figure 4. **Ribbon determinants are localized to the Golgi.** (A–L) Rescue of the ribbon by coinjection of Golgi extract with tubulin. Tubulin alone (A–D) or Golgi extract without (E–H) or with tubulin (I–L) were microinjected into the cytoplasts (asterisks). After 2 h of incubation, cells were stained for GFP (B, F, and J), tubulin (C, G, and K), and DNA (D, H, and L). Injection of tubulin or Golgi extract alone had no effect (B and F, asterisks), whereas Golgi extract together with tubulin reconstituted a Golgi ribbon (J, asterisk). Karyoplasts are marked by arrows. Bar, 10 μm. (M) Distribution of Golgi elements in the injected cytoplasts. A ribbon is formed if the Golgi is in no more than three continuous structures. (N) Equal amounts of protein (4 μg) of rat liver homogenate (H), cytosol (C), intermediate fraction (I), and Golgi membranes (RLG) were immunoblotted for the Golgi proteins GM130 and GRASP65, nuclear pore complex protein Nup153, ER enzyme PDI, motor protein dynein, and centrosome marker pericentrin. GM130 and GRASP65 were highly enriched on RLG membranes, whereas Nup153, PDI, dynein, and pericentrin were not detectable. (O) Medial/trans-Golgi proteins are enriched in the detergent extract. RLG membranes were extracted with *n*-octylglucoside, cleared by centrifugation (pellet [P]), and the supernatant was dialyzed to remove the detergent (S). Equal volumes of each fraction were immunoblotted for the indicated proteins. Cis-Golgi proteins were de-enriched (e.g., Golgin84, GM130, and GRASP65), whereas markers of the medial/trans-Golgi and the TGN were enriched in the extract (e.g., Golgin45, GRASP55, Vti1a, and TGN38). MT, microtubule; RSA, rat serum albumin.

and Video 2), which allowed partial incorporation of spindle materials into the cytoplasts, as revealed by the presence of a microtubule network (Fig. 5 G). Furthermore, a Golgi ribbon reformed (n = 21; Fig. 5 F), suggesting that ribbon determinants were segregated into the cytoplasts. Therefore, these data support the idea that ribbon factors are bound to and partitioned together with the spindle.

In metaphase, Golgi membranes decorate the spindle poles, suggesting that the spindle might regulate Golgi partitioning (Jokitalo et al., 2001). By uncoupling cytokinesis from chromosome segregation, we have demonstrated that the spindle directly partitions the factors required for Golgi ribbon assembly, thus extending the role of the spindle beyond chromosome segregation. In addition, our approach provides a potential avenue for investigating the nature of cytoplasm in vivo and free from the influence of the nucleus. In our case, the cytoplasts contained all the machinery required for protein synthesis (i.e., ribosomes) and exocytosis (i.e., ER and Golgi).

The cytoplasts received Golgi stacks capable of secretion independently of the spindle, but these stacks were not linked into a ribbon. This is in contrast to the karyoplasts, in which a ribbon reformed. Collectively, our data suggest two distinct mechanisms underlying Golgi inheritance. First, minimum functional Golgi units (stacks) are inherited in a spindle-independent manner. These stacks could be derived from Golgi that was partitioned together with the ER (Zaal et al., 1999) or could have reassembled from the Golgi that was segregated independently of the spindle (Jesch et al., 2001). Second, the mitotic spindle plays a vital role in transmitting ribbon determinants into the daughter cells.

The appearance of the Golgi ribbon in higher organisms during evolution reflects a different mechanism for polarized

Downloaded from http://rupress.org/jcb/article-pdf/184/3/391/1897081/jcb_200809090.pdf by guest on 09 February 2026

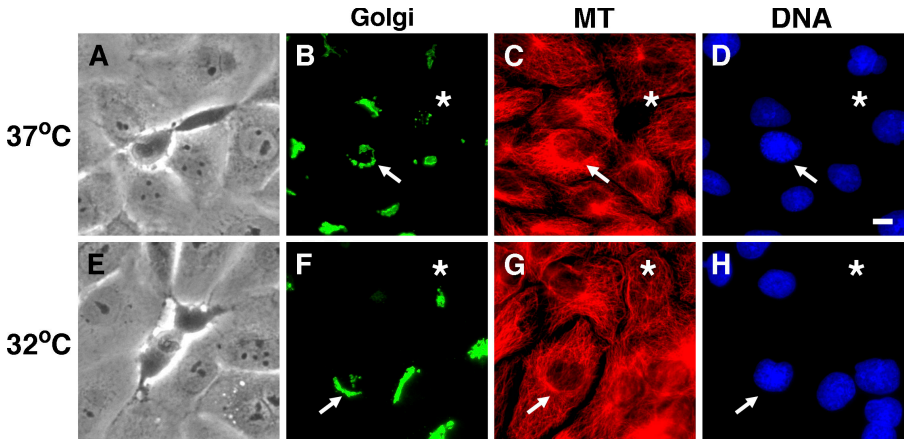

Figure 5. **Ribbon determinants partition together with the spindle.** Rescue of the ribbon by incorporation of spindle materials. Cells induced to divide asymmetrically at 37°C (A–D and Video 1, available at http://www.jcb.org/cgi/content/full/jcb.200809090/DC1) or 32°C (E–H and Video 2) were followed by video microscopy and stained for GFP (B and F), tubulin (C and G), and DNA (D and H). At 37°C, the spindle was located distal to the division plane (A). Microtubules (MT) were not partitioned into the cytoplasts (C, asterisk), and the Golgi was scattered (B, asterisk). At 32°C, the spindle was positioned close to the cleavage furrow (E). Spindle microtubules were incorporated into the cytoplasts (G, asterisk), and a Golgi ribbon reformed (F, asterisk). Karyoplasts are marked by arrows, and asterisks indicate cytoplasts. Bar, 10 µm.

secretion. In lower animals such as *Drosophila melanogaster*, Golgi stacks are scattered and localized adjacent to ER exit sites despite the presence of centrosomes. Polarized secretion is achieved by targeting mRNA to specific ER exit sites where the cargo is made and secreted locally (Herpers and Rabouille, 2004). However, in mammalian cells, cargo is posttranslationally sorted from the centrally located Golgi ribbon (for review see Bard and Malhotra, 2006). To establish cell polarity, the entire Golgi ribbon is reoriented toward the site of secretion (Bisel et al., 2008), which is essential for a variety of cellular processes such as the outgrowth of dendrites in neurons (Horton et al., 2005), fibroblast migration during wound healing (Preisinger et al., 2004), and the immune response (Stinchcombe et al., 2006). Because the ribbon is particularly important for more advanced functions, tight coupling of ribbon determinants with the spindle ensures that each daughter cell receives the information to assemble it. This might be the reason that mammalian cells use the highly regulated spindle apparatus to partition these factors instead of a stochastic ER-dependent process.

Materials and methods

Antibodies

The following antibodies were used: mouse monoclonal antibodies against GM130, Golgin84, TGN38, GS15, GS28, Vti1a (BD), CD8 (Wang et al., 2008), α-tubulin (TAT1; provided by K. Gull, University of Oxford, Oxford, England, UK), FITC-conjugated α-tubulin (DM1A; Sigma-Aldrich), dynein intermediate chains (74.1; Millipore), and nuclear pore complex (Mab414; Abcam). Rabbit polyclonal antibodies against GFP, S1P (Bartz et al., 2008), GRASP65 (provided by Y. Wang, University of Michigan, Ann Arbor, MI), p115 (provided by N. Nakamura, Kanazawa University, Kanazawa, Japan), pericentrin (Abcam), PDI (Assay Designs), Man I (provided by F. Barr, University of Liverpool, Liverpool, England, UK), Man II (provided by G. Warren, University of Vienna, Vienna, Austria), β-COP (EAGE; provided by R. Pepperkok, European Molecular Biology Laboratory, Heidelberg, Germany), p24γ3 (provided by T. Nielsson, University of Gothenburg, Gothenburg, Sweden), syntaxin 5 (provided by A. Price, Yale University, New Haven, CT), Rab1, giantin (provided by M. Beard, Yale University, New Haven, CT), Rab6, and myc (Santa Cruz Biotechnology, Inc.) were used. Sheep polyclonal antibodies against rat serum albumin (provided by G. Warren) were used. Polyclonal antibodies were raised in rabbits against GST fusion proteins of mouse Golgin45 (residues 1–123), rat GRASP55 (residues 232–454), and rat GM130 (residues 1–73 [N73]). N73-specific antibodies were affinity purified using His-tagged N73 covalently attached to *N*-hydroxysuccinimide–activated Sepharose (GE Healthcare). Goat anti–rabbit and goat anti–mouse antibodies conjugated to Alexa Fluor 488, 555, 594, or 647 were obtained from Invitrogen, and HRP-conjugated secondary antibodies were obtained from Thermo Fisher Scientific.

Cell line, tissue culture conditions, and drug treatments

Rat kangaroo kidney cells (PtK1) stably expressing NAGT I–GFP (Jokitalo et al., 2001) were grown in medium A (F-12 medium, 100 U/ml penicillin, 100 µg/ml streptomycin, 2 mM glutamine (Invitrogen), and 10% cosmic calf serum [HyClone]) with 300 µg/ml G418 (EMD) at 37°C and 5% CO_2. For live cell imaging, microinjections, immunofluorescence, and EM, PtK1 cells were grown on glass coverslips coated with Alcian blue 8GX (Sigma-Aldrich). To arrest cells in mitosis with monoasters, PtK1 cells were incubated for 2 h with an inhibitor of the kinesin Eg5, either 200 µM monastrol (BIOMOL International L.P.) or 20 µM S-trityl-L-cysteine (Acros Organics). To induce cell division, a Cdk1 inhibitor, either 50 µM roscovitine (EMD) or 25 µM purvalanol A (EMD), was added to medium. Microinjections of CD8 or myc–PDGF receptor mRNA and tubulin and/or Golgi extract were performed 2 h after addition of purvalanol A.

Protein purification and Golgi extraction

The oligomerization and Mad2-binding domain of Mad1 (residues 321–556; Canman et al., 2003) was cloned from IMAGE clone 4299982 (American Type Culture Collection) into pGEX4-T3 (GE Healthcare) purified on glutathione–Sepharose 4B (GE Healthcare), dialyzed against injection buffer (20 mM Hepes, pH 7.4, and 50 mM KOAc), and concentrated on a filter unit (Centricon YM-30; Millipore).

RLG membranes were purified as described previously (Wang et al., 2008). In brief, rat liver was homogenized in 0.5 M sucrose in PM buffer (potassium phosphate, pH 6.7, and 5 mM $MgCl_2$) with protease inhibitor cocktail (Roche). The homogenate was layered on top of 0.86 M sucrose, overlaid with 0.25 M sucrose, and centrifuged for 60 min at 29,000 rpm in a rotor (SW-41; Beckman Coulter). The 0.5 M sucrose layer was collected (cytosol fraction). The interface between the 0.5 and 0.86 M sucrose (intermediate fraction) was diluted to 0.25 M sucrose and layered on top of 1.3 and 0.5 M sucrose. After centrifugation for 30 min at 8,000 rpm in a rotor (SW-41), the enriched RLG membranes were collected at the 0.5/1.3 M sucrose interface. For microinjection experiments, RLG membranes were pelleted by centrifugation at 13,000 rpm for 10 min at 4°C, washed three times with injection buffer, extracted for 15 min on ice with 10% *n*-octylglucoside (EMD), and centrifuged at 13,000 rpm for 10 min at 4°C. The pellet was solubilized in sample buffer (pellet fraction), and the supernatant was dialyzed (10-kD cut off) against injection buffer (supernatant fraction), centrifuged again, and concentrated on a filter unit (Centricon YM-10; Millipore). Tubulin purified from bovine brain was provided by M. Kikkawa (Kyoto University, Kyoto, Japan).

In vitro transcription of mRNA

The expression plasmid pDprotA was generated by subcloning the coding sequence of protein A into pDisplay (Invitrogen) between the signal sequence and the myc epitope followed by the transmembrane domain of the PDGF receptor. Linearized pCD8 (Wang et al., 2008) and pDprotA were transcribed in vitro using the mMESSAGE mMachine T7 Ultra kit (Applied Biosystems). Capping, poly(A)-tailing reactions, and recovery of the mRNAs by LiCl precipitation were performed according to the manufacturer's instructions.

Downloaded from http://rupress.org/jcb/article-pdf/184/3/391/1897081/jcb_200809090.pdf by guest on 09 February 2026

Microinjection and live cell imaging

For time-lapse microscopy and microinjection experiments, cells were incubated in medium A containing 50 mM Hepes, pH 7.4. Microinjection was performed with a microinjector (Transjector 5246 or FemtoJet; Eppendorf) and a micromanipulator (5171; Eppendorf) connected to a microscope (Axiovert 200M; Carl Zeiss, Inc.; Bartz and Seemann, 2008). The reagents were injected at the following concentrations: 1.5 mg/ml Mad1 or Sar1dn (Bartz and Seemann, 2008), 0.2 mg/ml pCD8, 0.5 mg/ml CD8 or myc–PDGF receptor mRNA, 6 mg/ml tubulin, and 20 mg/ml Golgi extract. Mad1 was injected together with 2.5 mg/ml biotin-dextran as an injection marker and visualized by streptavidin–Alexa Fluor 350 (Invitrogen). All microinjection experiments were performed at least three times.

For time-lapse microscopy, coverslips were mounted into a chamber (Ludin; Life Imaging Services). The temperature was maintained using an incubator (XL-3; Carl Zeiss, Inc.) at 37°C unless otherwise stated. Phase-contrast images were taken at intervals of 3–20 min with an A-Plan 20×/0.3 PH1 objective (Carl Zeiss, Inc.) and a microscope (Axiovert 200M). Either a camera (Orca-285; Hamamatsu Photonics) and Openlab software (version 4.0.2; PerkinElmer) or a camera (DXM1200F; Nikon) in combination with MetaMorph software (version 7.1.3; MDS Analytical Technologies) was used.

Immunofluorescence and EM analysis

Cells were either fixed in 3.7% formaldehyde in PBS for 15 min and permeabilized in methanol at −20°C for 15 min or fixed and permeabilized in methanol at −20°C for 15 min and incubated with appropriate primary antibodies followed by secondary antibodies. DNA was stained with DRAQ5 (Biostatus) after RNase treatment or with Hoechst 33342 (Invitrogen). After staining, cells were mounted in Mowiol 4–88 (EMD). Upon the acquisition of time-lapse phase-contrast images, cells were fixed and stained in the chamber (Ludin) and repositioned onto the microscope stage to the original positions recorded during live cell imaging. Immunofluorescence analysis was performed with a Plan Neofluar 40×/1.3 differential interference contrast objective (Carl Zeiss, Inc.) and a camera (Orca-285) with the Openlab software (version 4.0.2). The contrast of the images was adjusted for the Golgi structures in the cytoplasts.

For quantitative analysis of the ribbon structure, the analyze particles function of ImageJ (National Institutes of Health) was used, and a fixed threshold was applied to all raw images (Puthenveedu et al., 2006). The Golgi was determined as a ribbon if 90% of the fluorescence intensity resided in no more than three continuous elements.

EM analysis was performed essentially as described previously (Wang et. al, 2008). Asymmetrical cell division was induced by treatment with trityl-cysteine (2 h) followed by purvalanol A (2 h) and monitored by video microscopy. Upon division, the cells surrounding the karyoplasts and cytoplasts were scraped off with a microinjection needle. The remaining cells were fixed in 2.5% glutaraldehyde in 0.1 M sodium cacodylate, pH 7.4, for 30 min, treated with 1% osmium tetroxide and 1.5% potassium cyanoferrate in 0.1 M cacodylate for 30 min, and embedded in Epon 812 (Electron Microscopy Sciences). Upon removal of the coverslips by hydrofluoric acid, thin sections were cut and stained with 2% uranyl acetate and lead citrate. Sections were analyzed on an electron microscope (Tecnai G2 Spirit; FEI Company), and images were captured on a charge-coupled device camera (USC1000 2k; Gatan). Stacks were defined as three or more cisternae separated by <20 nm.

Online supplemental material

Fig. S1 shows transport of newly synthesized proteins to the cell surface. Fig. S2 shows that temperature affects spindle positioning during division. Video 1 shows that PtK1 cells were induced to divide asymmetrically at 37°C. Video 2 shows that PtK1 cells were induced to divide asymmetrically at 32°C. Online supplemental material is available at http://www.jcb.org/cgi/content/full/jcb.200809090/DC1.

We thank C. Gilpin, T. Januszewski, and the University of Texas Southwestern EM facility for EM assistance, Y. Wang, D. Mundy, and B. Bisel for critical reading of the manuscript, M. Kikkawa for purified tubulin, and H. Yu for advice.

J. Seemann is a Virginia Murchison Lithicum Scholar in Medical Research and is supported by a grant from the American Heart Association (0806090F).

Submitted: 12 September 2008
Accepted: 7 January 2009

References

Bard, F., and V. Malhotra. 2006. The formation of TGN-to-plasma-membrane transport carriers. *Annu. Rev. Cell Dev. Biol.* 22:439–455.

Bartz, R., and J. Seemann. 2008. Mitotic regulation of SREBP and ATF6 by separation of the Golgi and ER. *Cell Cycle.* 7:2100–2105.

Bartz, R., L.P. Sun, B. Bisel, J.H. Wei, and J. Seemann. 2008. Spatial separation of Golgi and ER during mitosis protects SREBP from unregulated activation. *EMBO J.* 27:948–955.

Bisel, B., Y. Wang, J.H. Wei, Y. Xiang, D. Tang, M. Miron-Mendoza, S. Yoshimura, N. Nakamura, and J. Seemann. 2008. ERK regulates Golgi and centrosome orientation towards the leading edge through GRASP65. *J. Cell Biol.* 182:837–843.

Canman, J.C., L.A. Cameron, P.S. Maddox, A. Straight, J.S. Tirnauer, T.J. Mitchison, G. Fang, T.M. Kapoor, and E.D. Salmon. 2003. Determining the position of the cell division plane. *Nature.* 424:1074–1078.

Diao, A., D. Rahman, D.J. Pappin, J. Lucocq, and M. Lowe. 2003. The coiled-coil membrane protein golgin-84 is a novel rab effector required for Golgi ribbon formation. *J. Cell Biol.* 160:201–212.

Herpers, B., and C. Rabouille. 2004. mRNA localization and ER-based protein sorting mechanisms dictate the use of transitional endoplasmic reticulum-golgi units involved in gurken transport in *Drosophila* oocytes. *Mol. Biol. Cell.* 15:5306–5317.

Horton, A.C., B. Rácz, E.E. Monson, A.L. Lin, R.J. Weinberg, and M.D. Ehlers. 2005. Polarized secretory trafficking directs cargo for asymmetric dendrite growth and morphogenesis. *Neuron.* 48:757–771.

Hu, C.K., M. Coughlin, C.M. Field, and T.J. Mitchison. 2008. Cell polarization during monopolar cytokinesis. *J. Cell Biol.* 181:195–202.

Jesch, S.A., A.J. Mehta, M. Velliste, R.F. Murphy, and A.D. Linstedt. 2001. Mitotic Golgi is in a dynamic equilibrium between clustered and free vesicles independent of the ER. *Traffic.* 2:873–884.

Jokitalo, E., N. Cabrera-Poch, G. Warren, and D.T. Shima. 2001. Golgi clusters and vesicles mediate mitotic inheritance independently of the endoplasmic reticulum. *J. Cell Biol.* 154:317–330.

Lowe, M., and F.A. Barr. 2007. Inheritance and biogenesis of organelles in the secretory pathway. *Nat. Rev. Mol. Cell Biol.* 8:429–439.

Maniotis, A., and M. Schliwa. 1991. Microsurgical removal of centrosomes blocks cell reproduction and centriole generation in BSC-1 cells. *Cell.* 67:495–504.

Mayer, T.U., T.M. Kapoor, S.J. Haggarty, R.W. King, S.L. Schreiber, and T.J. Mitchison. 1999. Small molecule inhibitor of mitotic spindle bipolarity identified in a phenotype-based screen. *Science.* 286:971–974.

Niiya, F., X. Xie, K.S. Lee, H. Inoue, and T. Miki. 2005. Inhibition of cyclin-dependent kinase 1 induces cytokinesis without chromosome segregation in an ECT2 and MgcRacGAP-dependent manner. *J. Biol. Chem.* 280:36502–36509.

Pelletier, L., E. Jokitalo, and G. Warren. 2000. The effect of Golgi depletion on exocytic transport. *Nat. Cell Biol.* 2:840–846.

Preisinger, C., B. Short, V. De Corte, E. Bruyneel, A. Haas, R. Kopajtich, J. Gettemans, and F.A. Barr. 2004. YSK1 is activated by the Golgi matrix protein GM130 and plays a role in cell migration through its substrate 14-3-3ζ. *J. Cell Biol.* 164:1009–1020.

Puthenveedu, M.A., C. Bachert, S. Puri, F. Lanni, and A.D. Linstedt. 2006. GM130 and GRASP65-dependent lateral cisternal fusion allows uniform Golgi-enzyme distribution. *Nat. Cell Biol.* 8:238–248.

Shima, D.T., K. Haldar, R. Pepperkok, R. Watson, and G. Warren. 1997. Partitioning of the Golgi apparatus during mitosis in living HeLa cells. *J. Cell Biol.* 137:1211–1228.

Shima, D.T., N. Cabrera-Poch, R. Pepperkok, and G. Warren. 1998. An ordered inheritance strategy for the Golgi apparatus: visualization of mitotic disassembly reveals a role for the mitotic spindle. *J. Cell Biol.* 141:955–966.

Skoufias, D.A., S. Debonis, Y. Saoudi, L. Lebeau, I. Crevel, R. Cross, R.H. Wade, D. Hackney, and F. Kozielski. 2006. S-trityl-l-cysteine is a reversible, tight-binding inhibitor of the human kinesin eg5 that specifically blocks mitotic progression. *J. Biol. Chem.* 281:17559–17569.

Stinchcombe, J.C., E. Majorovits, G. Bossi, S. Fuller, and G.M. Griffiths. 2006. Centrosome polarization delivers secretory granules to the immunological synapse. *Nature.* 443:462–465.

Wang, Y., J.H. Wei, B. Bisel, D. Tang, and J. Seemann. 2008. Golgi cisternal unstacking stimulates COPI vesicle budding and protein transport. *PLoS ONE.* 3:e1647.

Zaal, K.J., C.L. Smith, R.S. Polishchuk, N. Altan, N.B. Cole, J. Ellenberg, K. Hirschberg, J.F. Presley, T.H. Roberts, E. Siggia, et al. 1999. Golgi membranes are absorbed into and reemerge from the ER during mitosis. *Cell.* 99:589–601.

Downloaded from http://rupress.org/jcb/article-pdf/184/3/391/1897081/jcb_200809090.pdf by guest on 09 February 2026